

Structural Analysis And Topology Optimization Design For Bandwidth Extension of Magnetolectric Seismometer

Zhenjing Yao (✉ yaozhenjing000@126.com)

Institute of Disaster Prevention

Jingyi Zhang

Institute of Disaster Prevention

Zhitao Gao

Institute of Disaster Prevention

Yaran Liu

Institute of Disaster Prevention

Mingyang Li

Institute of Disaster Prevention

Research Article

Keywords: Seismometer, Frequency bandwidth, Natural frequency, Spurious frequency, Topology optimization

Posted Date: November 18th, 2021

DOI: <https://doi.org/10.21203/rs.3.rs-1037972/v1>

License:   This work is licensed under a Creative Commons Attribution 4.0 International License.

[Read Full License](#)

Structural analysis and topology optimization design for bandwidth extension of magnetoelectric seismometer

Zhenjing Yao^{a,b} Jingyi Zhang^{a,b} Zhitao Gao^{a,b} Yaran Liu^{a,b} Mingyang Li^{a,b}

a Institute of Disaster Prevention, Sanhe 065201, China

b Hebei Key Laboratory of Seismic Disaster Instrument and Monitoring Technology, Sanhe 065201, China

ABSTRACT

Magnetoelectric seismometers can measure earthquake information and play an important role in earthquake monitoring. Aiming at the wider effective frequency bandwidth of magnetoelectric seismometers, a novel seismometer based on topology optimization structural pendulum is reported. The topology optimization of leaf spring structure in magnetoelectric seismometer is designed, the natural frequency and spurious frequency characteristics of the novel seismometer are analyzed. Based on variable density theory, the Solid Isotropic Material with Penalization (SIMP) model of the seismometer is established, and the Method of Moving Asymmetric (MMA) is adopted to obtain the optimal topology structure. The finite element analysis using ANSYS shows that novel seismometer after topology optimization structure is characteristic with lower natural frequency and higher spurious frequency than that of before optimization seismometer. The real vibration experimental results indicate that after topology optimization, the effective frequency bandwidth of seismometer is increased by 55.50%, improving from [1s, 51Hz] to [4s, 78Hz].

Keywords: Seismometer, Frequency bandwidth, Natural frequency, Spurious frequency, Topology optimization.

1. Introduction

Seismometers, as ground motion measurement instruments, have been widely used in geological hazard predictions, earthquake early warning, engineering exploration and nuclear explosions monitoring [1-4]. A seismometer can turn ground velocity within a certain bandwidth into an electric output signal without distortion [5]. The response signal of seismometer will decline or become distorted when it falls below natural frequency or near spurious frequency. Therefore, seismometers with a lower natural frequency and a higher spurious frequency play an important role in ground motion measurements with wider bandwidth, ensuring the reliability of quality data acquisition.

The structural changes in leaf spring of seismometer can search for lower natural frequency and higher spurious frequency with wider effective frequency bandwidth to a certain extent. Faber and Maxwell alter the leaf spring structure of a seismometer to increase spurious frequency which can expand its frequency bandwidth [6]. Woo invents inner and outer annular rings connected by spring arm for a seismometer, which improves the ratio between spurious frequency and natural frequency to broaden bandwidth and reduce signal distortion [7]. Wielandt and Streckeisen propose a seismometer with a rectangular leaf spring instead of a zero-length helical spring, which has a broader bandwidth [8]. Yang *et al.* adopt multiple pairs of leaf springs in a suspension system for a seismometer, which increases the ratio of

33 spurious frequency to natural frequency in order to expand its frequency range [9]. Xin *et al.* design a multilayer
34 spiral-corrugated cantilever beam for a piezoelectric seismometer, which has a lower natural frequency [10]. Yao *et al.*
35 propose a novel leaf spring as a substitute for traditional spring to expand effective bandwidth of a seismometer [11]. The
36 existing topology structure of original leaf spring can search for lower natural frequency and higher spurious frequency
37 in a certain extent. However, the topology structure of leaf spring cannot be optimized which has a large space for
38 expanding bandwidth of a seismometer.

39 This paper demonstrates how the novel seismometer with topology optimization leaf spring structure can improve the
40 effective frequency bandwidth. The proposed topology optimization leaf spring structure with lower natural frequency
41 and higher spurious frequency can broaden frequency bandwidth. Based on variable density theory, the Solid Isotropic
42 Material with Penalization (SIMP) model of seismometer is established, and the Method of Moving Asymmetric (MMA)
43 is adopted to obtain the optimal topology structure. As well as the natural frequency and spurious frequency
44 characteristics of novel topology optimization structure seismometer are analyzed. The finite element simulation analysis
45 using ANSYS Workbench 19.0 and real measurement experiments are conducted to confirm validity of the design.

46 The rest of this paper is structured as follows: The working principles are explained in Sec. 2; Sec. 3 presents structural
47 analysis; Topology optimization and design of novel topology seismometer is introduced in Sec. 4 and Sec. 5; Sec. 6
48 illustrates finite element simulation analysis; Sec. 7 represents experiments and discussions, and conclusions in Sec.8.

49 **2. Working principles**

50 The ground motion measurement can directly sense by the mechanical pendulum of seismometer [12]. It suspends an
51 inertial reference mass structure from a rigid fixed shell structure, which is connected by a leaf spring. When local
52 seismic waves occur, the fixed shell structure coupled with the ground vibrates immediately. The inertial reference mass
53 still tends to remain static, so the relative movement is generated between mass and shell. Using this relative motion, the
54 ground motion can be measured. As shown in Fig. 1, the pendulum of seismometer can be simplified as a
55 mass-spring-damping mechanical model.

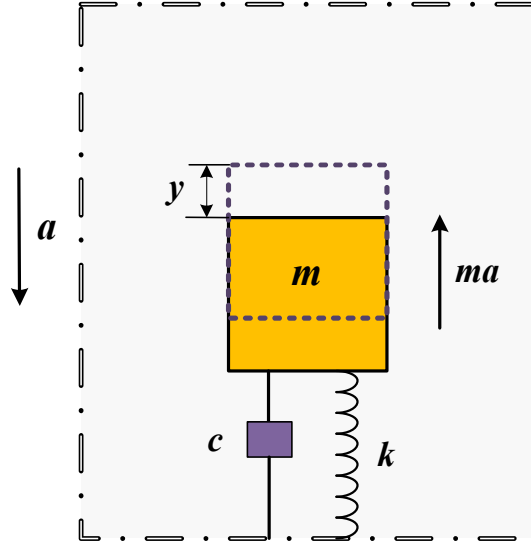


Fig. 1. Model of the mechanical pendulum

Under the ideal conditions, when the displacement of ground motion Y produces relative displacement y between the mass and shell, the motion equation of mechanical pendulum can be shown as

$$m \frac{d^2 y}{dt^2} + c \frac{dy}{dt} + ky = m \frac{d^2 Y}{dt^2} \quad (1)$$

Wherein, m represents the quality of inertial reference mass structure, k is the stiffness of connecting leaf spring, and c represents the damping coefficient of mechanical pendulum.

Assuming that damping can be neglected, the mechanical pendulum vibrates in simple harmonic. With finite element discretization of the mechanical pendulum vibration motion, after element analysis and boundary condition, the motion equation with finite element of mechanical pendulum can be represented as

$$\mathbf{M}\ddot{\mathbf{y}} + \mathbf{K}\mathbf{y} = \mathbf{0} \quad (2)$$

Where \mathbf{M} and \mathbf{K} are the mass matrix and stiffness matrix of mechanical pendulum, respectively. \mathbf{y} and $\ddot{\mathbf{y}}$ are the displacement vector and acceleration vector of mechanical pendulum, respectively.

When the mechanical pendulum vibrates in simple harmonic, the natural vibration frequency equation of the mechanical pendulum can be shown as follows,

$$(\mathbf{K} - \omega^2 \mathbf{M})\Phi = \mathbf{0} \quad (3)$$

Where ω represents the vibration angular frequency of mechanical pendulum, and feature vector Φ is the vibration mode of mechanical pendulum.

In this way, the j -order frequency f_j of mechanical pendulum can be expressed as

$$f_j = \frac{1}{2\pi} \sqrt{\frac{\Phi_j^T \mathbf{K} \Phi_j}{\Phi_j^T \mathbf{M} \Phi_j}} \quad (4)$$

Where Φ_j is feature vector related to the j -order angular frequency of mechanical pendulum. As can be seen from equation (4), the j -order frequency of mechanical pendulum depends only on the stiffness matrix \mathbf{K} and the mass matrix \mathbf{M} . Order to minimize natural frequency and maximize spurious frequency of mechanical pendulum, structural analysis and design of topology optimization leaf spring in rectangle structure is considered, which can change the stiffness matrix and mass matrix of mechanical pendulum.

3. Structural analysis

The working principle of magnetolectric seismometer is that the mechanical pendulum directly perceives the ground vibration, and the connected working coil cuts the magnetic induction line in the magnetic field, then converts the ground motion into electricity for measurement. The key structure of mechanical pendulum is composed of leaf spring, counterweight, beam, heavy hammer, coil support, large coil frame and pressure plate as shown in Fig 2.

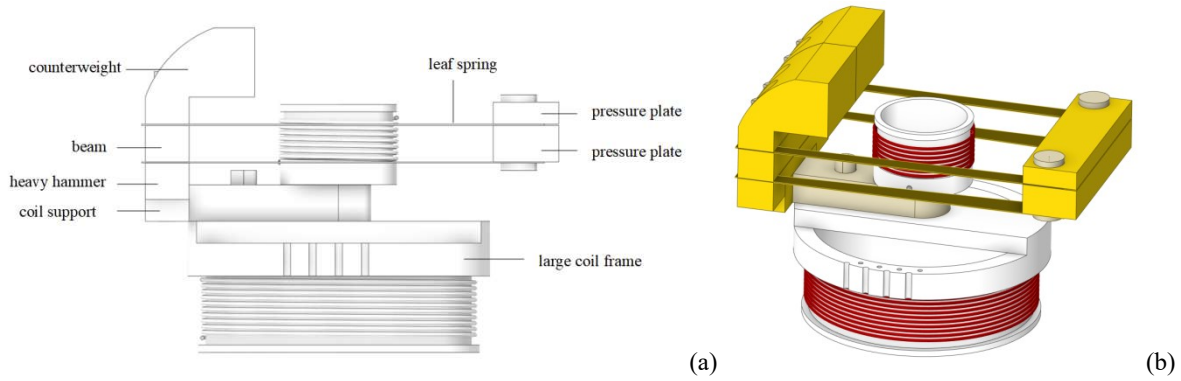


Fig. 2. (a) Structure of mechanical pendulum and (b) 3D diagram of mechanical pendulum in magnetolectric seismometer

The finite element analysis model of mechanical pendulum is built to study the influence of leaf spring size on the natural frequency and spurious frequency. After solid modeling, defining material property and meshing grid, the unit and node number in finite element model is set to 84349 and 148061, respectively. When seismometer measures the ground vibration, the hammer end connected by the leaf spring swing freely and the pressure plate end connected by the leaf spring is fixed. So it has fixed constraints on the end of pressure plate. Loading the stand earth gravity, the finite element analysis of mechanical pendulum is carried out. The first order modal shape and the second order modal shape of mechanical pendulum is shown in Figure 3. It can be seen from Fig. 3(a) that the main vibration of the first order modal of mechanical pendulum is bending motion, while the main vibration of the second order modal of mechanical pendulum is twisting motion in Fig. 3(b). In the seismometer measurement, the actual motion of the mechanical

97 pendulum is the up and down variation, while the twisting motion is the unexpected motion. Moreover, the excessive
98 twisting motion could destroy the mechanical pendulum, so it is necessary to has a lower natural frequency and higher
99 spurious frequency of the mechanical pendulum.

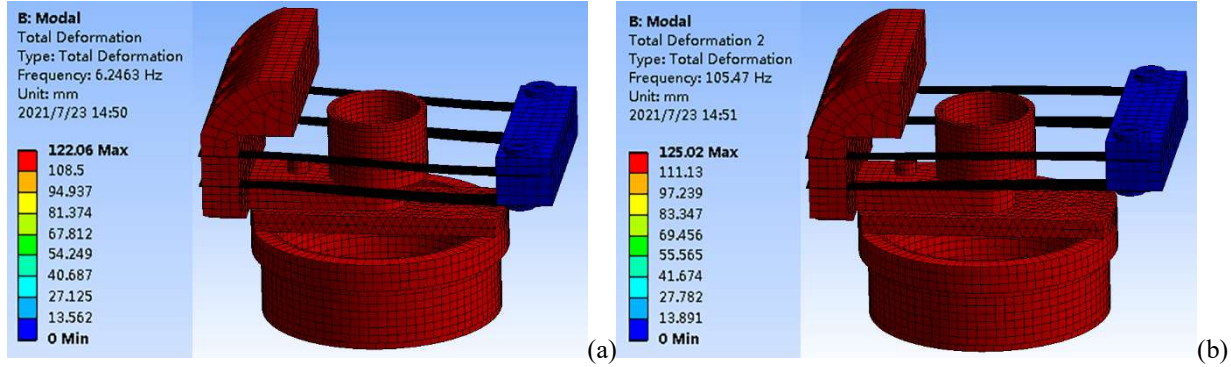
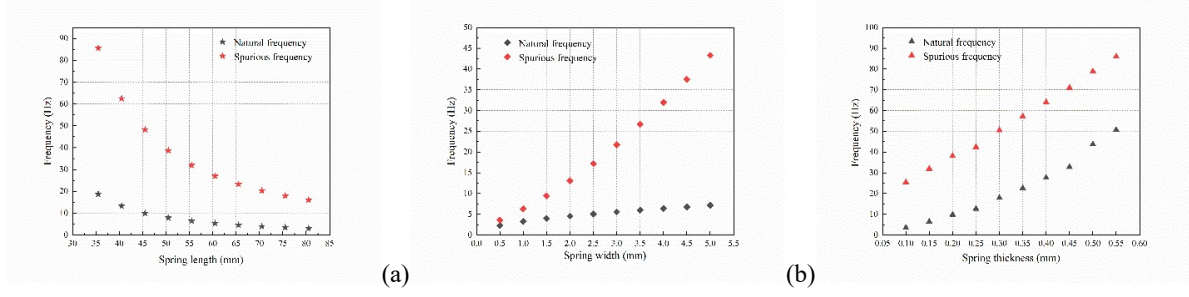


Fig. 3. The finite element analysis (a) the first order modal shape (b) the second order modal shape

102 The size of leaf spring is a key factor affecting the natural frequency and spurious frequency of mechanical
103 pendulum. In order to obtain the variation laws between the size and frequency of mechanical pendulum,
104 changing the length, width and thickness of leaf spring, the corresponding natural frequency and spurious
105 frequency of the mechanical pendulum are analyzed.

106 In finite element model of the mechanical pendulum, the length of the leaf spring is 30.00-85.00mm at
107 5.00mm interval, the width of the leaf spring is 0-5.50mm at 0.50mm interval, and the thickness of the leaf
108 spring is 0-0.55mm at 0.05mm interval. With the increase of the leaf spring length, the natural frequency of
109 the pendulum decreases from 18.71Hz to 3.04Hz, and the spurious frequency decreases from 85.49Hz to
110 16.04Hz, and the difference between the natural frequency and the spurious frequency of the mechanical
111 pendulum decreases from 66.78Hz to 12.99Hz as shown in Fig 4(a). With the increase of the spring width,
112 the natural frequency increases from 2.31Hz to 7.14Hz, the spurious frequency increases from 3.60Hz to
113 43.31Hz, and the difference between the natural frequency and the spurious frequency of the pendulum
114 increases from 1.29Hz to 36.17Hz as shown in Fig 4(b). With the thickness of the leaf spring increases from
115 0 to 0.55mm, the natural frequency of the pendulum increases from 3.49Hz to 50.63Hz and the spurious
116 frequency from 25.42Hz to 85.98Hz, and the difference between the natural frequency and the spurious
117 frequency of the pendulum increases from 21.93Hz to 35.35Hz as shown in Fig 4(c).



118

119 **Fig. 4.** The variation laws between the size and frequency of mechanical pendulum: (a) change in natural frequency and spurious frequency with spring length (b) change in natural frequency and spurious frequency with spring width (c) change in natural frequency and spurious frequency with spring thickness.

122 The increase in length of the leaf spring causes a rapid decrease in the difference between natural
 123 frequency and spurious frequency of the pendulum, while the increase in width of the leaf spring induces a
 124 rapid growth in the difference between natural frequency and spurious frequency of the pendulum, but the
 125 increase in thickness of the leaf spring has little effect on the difference between natural frequency and
 126 spurious frequency of the pendulum. In this study, the length of the leaf spring is set to 57.50mm, the width
 127 is 4.00mm, and the thickness is 0.15mm. The analysis result of the natural frequency is 6.24Hz, and the
 128 spurious frequency is 105.47Hz.

129 4. Topology optimization

130 In order to design seismometers with lower natural frequency and higher spurious frequency, a topology optimal
 131 structure of leaf spring is proposed. Topology optimization is to find the optimal distribution of materials in
 132 given area and boundary conditions [13,14]. Based on variable density theory, the Solid Isotropic Material
 133 with Penalization (SIMP) model of seismometer is established, and the problem of minimizing natural
 134 frequency of mechanical pendulum can be formulated as follows,

135

$$\begin{aligned}
 &\text{Find : } x = (x_1, x_2, \dots, x_N)^T \\
 &\min : f = \frac{1}{2\pi} \sqrt{\frac{\Phi_1^T \mathbf{K} \Phi_1}{\Phi_1^T \mathbf{M} \Phi_1}} \\
 &s.t. \quad (\mathbf{K} - \lambda \mathbf{M}) \Phi = \mathbf{0} \\
 &\quad \lambda = \eta f^2 \\
 &\quad \sum_{i=1}^N V_i x_i - V^* \leq 0 \\
 &\quad 0 \leq x_{\min} \leq x_i \leq 1
 \end{aligned} \tag{5}$$

136 Wherein x is the design variable, x_i is the unit density, and x_{\min} is the lower limit of the unit density. N
 137 represents the element number, V^* is the allowable volume of material, λ represents eigenvalue, and f is the
 138 natural frequency of mechanical pendulum.

139 The sensitivity of natural frequency in mechanical pendulum can be shown as follows,

$$\begin{aligned}
 140 \quad \frac{\partial f}{\partial x_i} &= \Phi_1^T \left(\frac{\partial \mathbf{K}}{\partial x_i} - f \frac{\partial \mathbf{M}}{\partial x_i} \right) \Phi_1 \\
 141 \quad \mathbf{K} &= \sum_{i=1}^N (E_{\min} + x_i^P (E_0 - E_{\min})) \mathbf{K}_i \\
 142 \quad \mathbf{M} &= \sum_{i=1}^N (E_{\min} + x_i^P (E_0 - E_{\min})) \mathbf{M}_i
 \end{aligned} \tag{6}$$

143 Where P is the penalty factor for intermediate density materials, E_0 and E_{\min} are the elastic modulus of materials in
 144 material region and hole region, respectively. \mathbf{K}_i and \mathbf{M}_i are the stiffness and mass of i -th element, respectively.

145 The Method of Moving Asymptote (MMA) is adopted to solve topology optimization problem with SIMP
 146 model of seismometer. MMA is a convex approximate linearization method based on the first derivative
 147 [15-20]. To improve algorithm performance, the artificial variables are introduced into the SIMP
 148 optimization model. The mathematical model can be expressed as follows,

$$\begin{aligned}
 149 \quad \min : & \frac{1}{2\pi} \sqrt{\frac{\Phi_1^T \mathbf{K} \Phi}{\Phi_1^T \mathbf{M} \Phi}} + a_0 z + \sum_{j=1}^m (c_j y_j + \frac{1}{2} d_j y_j^2) \\
 \text{s.t.} : & f_j(x) - a_j z - y_j \leq 0 \quad j=1, 2, \dots, m \\
 & x_i^{\min} \leq x_i \leq x_i^{\max} \quad i=1, 2, \dots, N \\
 & z \geq 0, \quad y_j \geq 0 \quad j=1, 2, \dots, m
 \end{aligned} \tag{7}$$

150 Where y and Z are artificial variables, $a_0, c_j, d_j, a_j, x_i^{\min}$ and x_i^{\max} are real number greater than zero, m is
 151 number of constraints.

152 The steps of MMA to solve seismometer topology optimization problem are that:

153 Step 1: Selecting the initial iteration point of design variables. The size of initial finite element in design
 154 domain is 9562.

155 Step 2: Calculating values of the natural frequency function and constraint function, and sensitivity of the
 156 natural frequency in mechanical pendulum at the current iteration point of design variable.

157 Step 3: Solving next iteration point of design variables. Generating MMA sub-problem with adding
 158 artificial variables, original dual method is used to solve the approximate solution as the next iteration point
 159 of design variables.

160 Step 4: Judging the termination conditions. If the convergence condition is met, acquiring the optimal
161 topology structure; if not, return to Step 2.

162 5. Design of novel topology optimization seismometer

163 Aiming to have a wider effective frequency bandwidth seismometer, we have designed novel seismometer using an
164 optimal topology leaf spring structure pendulum based on SIMP model and MMA algorithm. The design area of
165 mechanical pendulum is the blue area as shown in Fig. 5(a). For MMA optimization algorithm, the penalty factor is
166 taken to 3, the convergence accuracy is 0.1%. The main frequency of the central processing unit and random access
167 memory used for implementation of optimization algorithm are 2.6 Hz and 64 GB, respectively. With the size of initial
168 finite element in SIMP model is set to 9562 and maximum iteration number is set to 500 in MMA optimization
169 algorithm, the topology optimization structure leaf spring is as shown in Fig. 5(b). Adopting the topology optimization
170 structure leaf spring, the novel optimization pendulum for a seismometer is assembled. Figures 5(c)–5(d) illustrate the
171 exploded view of the novel optimization pendulum and the finite element model of the novel optimization pendulum,
172 respectively. The natural frequency of novel pendulum with topology optimization structure leaf spring is decreased to
173 3.21Hz, and the spurious frequency is 124.14Hz.

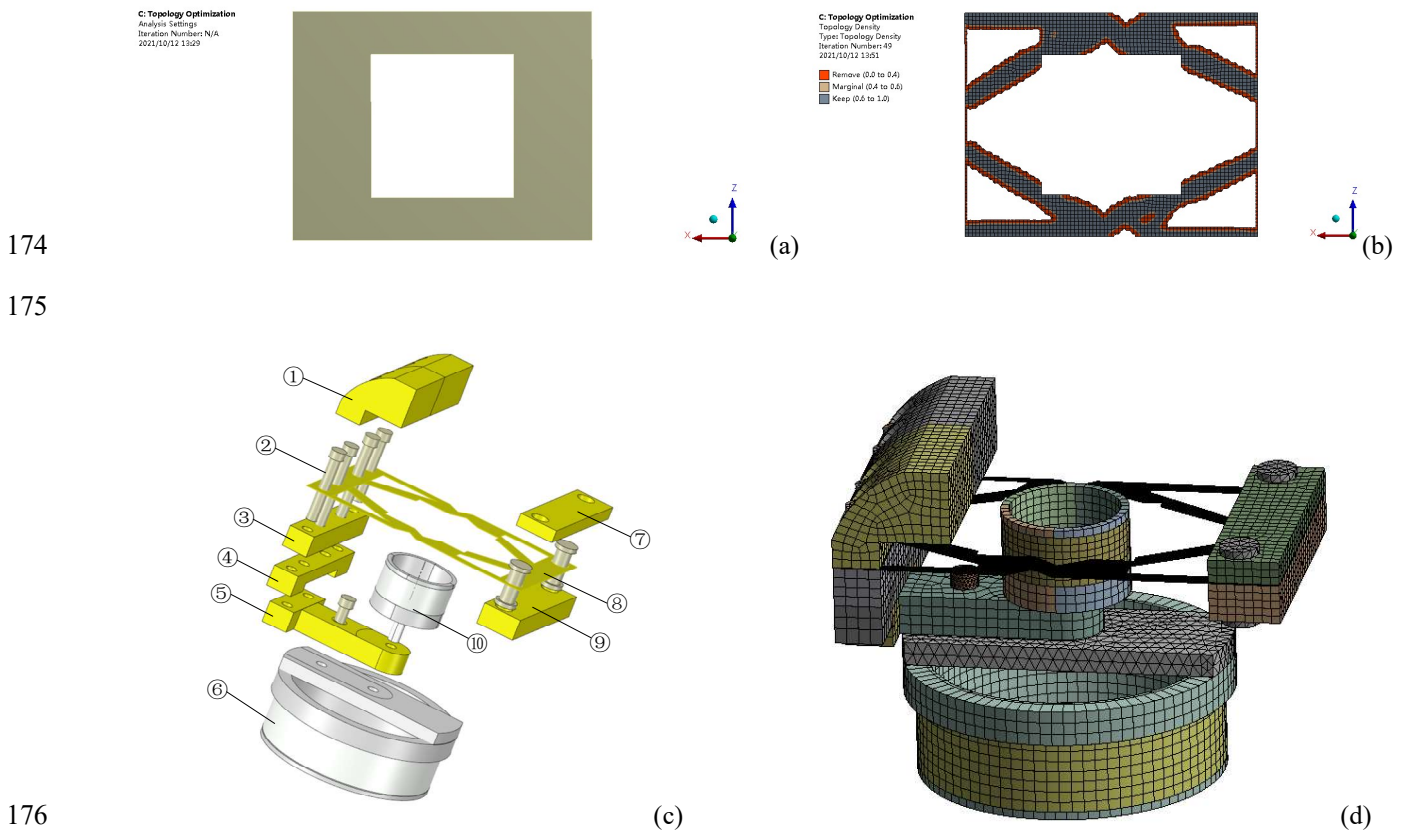


Fig. 5. Design of the novel seismometer with topology optimization (a) design area of mechanical pendulum; (b) topology optimization leaf spring structure; (c) exploded view of the novel topology pendulum is as follows: ① counterweight, ②

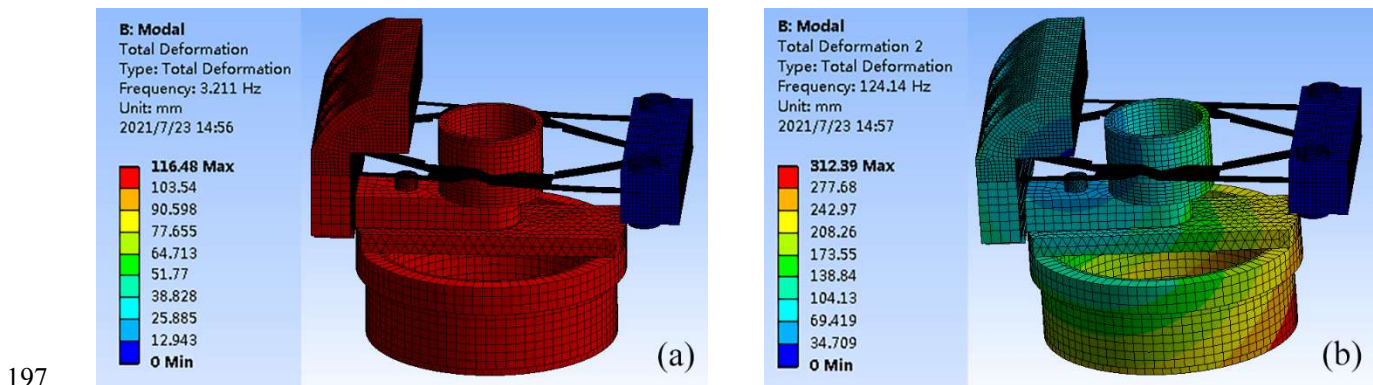
179 bolts, ③ beam, ④ heavy hammer, ⑤ coil support, ⑥ large coil frame, ⑦ pressure plate, ⑧ novel optimization leaf
180 spring, ⑨ pressure plate, ⑩ small coil frame; (d) finite element model of the novel optimization pendulum.

181 6. Finite element simulation analysis

182 In order to compare the performance of novel topology optimization leaf spring structure and before optimization leaf
183 spring structure for a seismometer, a finite element analysis using ANSYS Workbench 19.0 (finite element computer
184 program) is conducted. The finite element simulation experiments are carried out by a workstation. The main frequency
185 of central processing unit and the random access memory used for simulation are 2.6 Hz and 64 GB, respectively. The
186 modal analysis and harmonic response analysis are conducted on two pendulum structures. The natural frequency and
187 spurious frequency of pendulum structure for a seismometer are analyzed.

188 6.1 Modal analysis

189 In modal analysis, the natural frequency and spurious frequency of pendulum structure for a seismometer are analyzed
190 under free vibration. The first and second order modal shapes of novel topology optimization pendulum using modal
191 analysis under ANSYS Workbench are carried out. Figure 6(a) present the first order modal shape of novel topology
192 optimization pendulum. Figure 6(b) illustrate the second order modal shape of novel topology optimization pendulum.
193 From Fig. 6, we can observe that the direction of first order modal shape is concurrent with ground movement, but the
194 direction of second order modal shape is intersected with the ground variation, which can produce a spurious signal for a
195 seismometer. The natural frequency of novel pendulum with topology optimization leaf spring is 3.21Hz, and the
196 spurious frequency is 124.14Hz.



197
198 **Fig. 6.** Modal analysis results (a) The first order modal shape of the novel optimization optimization pendulum, (b) the second
199 order modal shape of the novel optimization pendulum.

200 Table 1 shows the natural frequency and spurious frequency of two kinds of pendulum. The natural frequency of novel
201 pendulum with topology optimization leaf spring is decreased with before optimization pendulum from 6.24 Hz to
202 3.21Hz, which is 48.55% reduction. Meanwhile, the spurious frequency of novel optimization pendulum is increased

203 with that of before optimization pendulum from 105.47Hz to 124.14Hz, which is 17.70% increase. The finite element
204 analysis shows that novel seismometer with topology optimization structure is characteristic with lower natural frequency
205 and higher spurious frequency than that of before optimization seismometer.

206 **Table 1** Natural frequency and spurious frequency of two kinds of pendulum.

	Natural frequency (Hz)	Spurious frequency (Hz)
Novel optimization pendulum	3.21	124.14
Before optimization pendulum	6.24	105.47

207 6.2 Harmonic response analysis

208 In harmonic response analysis, the natural frequency of pendulum structure for a seismometer are analyzed under
209 forced vibration. The amplitude frequency characteristics of novel topology optimization pendulum and before
210 optimization pendulum using harmonic response analysis under ANSYS Workbench are implemented. In simulation
211 experiment, the amplitude of input sine vibrational signals is 10N, and the frequency is 0-10 Hz at 0.2Hz intervals. The
212 harmonic response measurement results of novel topology optimization pendulum and before optimization pendulum are
213 illustrated in Fig. 7. It can be seen from Fig.7 that the maximum output stress of novel topology optimization pendulum
214 is 77.45MPa at 3.21Hz. And the output voltage of before optimization structure pendulum is 13.50MPa at 6.24Hz.
215 Compared with before optimization structure pendulum, the natural frequency of novel topology optimization pendulum
216 has reduced by about 48.55%, as well as the maximum output stress of novel topology optimization pendulum has
217 increased 4.7 times.

218

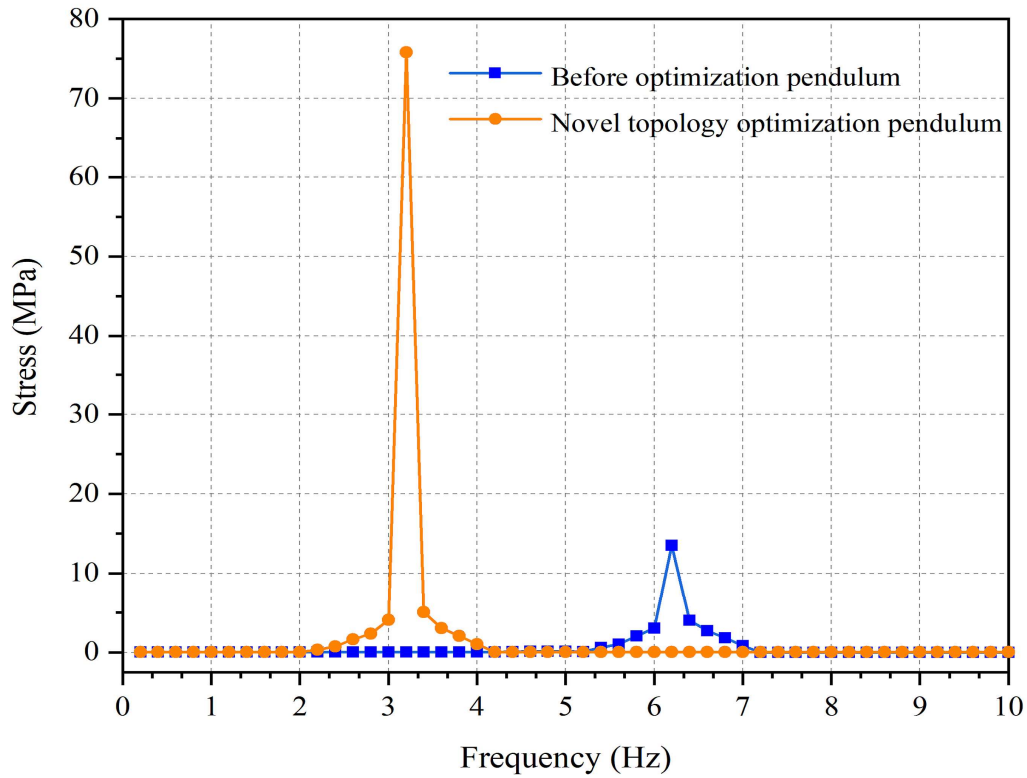


Fig. 7. Harmonic response analysis results of the two kinds of pendulum.

7. Experiments and discussions

7.1 Modal testing experiments

In order to validate theoretical and simulation results, the natural frequency and spurious frequency characteristics of two pendulum structures are measured in Hebei key laboratory of seismic disaster instrument and monitoring technology. Figure 8 shows the material object of novel structure pendulum with topology optimization leaf spring. The modal testing experiments using the Brüel & Kjær (BK) vibration test system is represented in Fig. 9. The force hammer knocks the pendulum at excitation points sticking accelerometers. After charge amplification, the vibration signal is obtained from the six-channel data collector. The signal modal analysis with BK pulse reflex modal fitting software can be determined at the workstation.



Fig.8. Material object of novel optimization structure pendulum

In the experiments, the 8206-002 series small force hammer is used as the vibration equipment. A BK type 3050-A-060 six-channel data collector, 4508-001 accelerometer and BK pulse labshop test system is adopted as test equipment. The number of excitation points is set to 20. And the sampling frequency of the data collector is set to 200Hz.

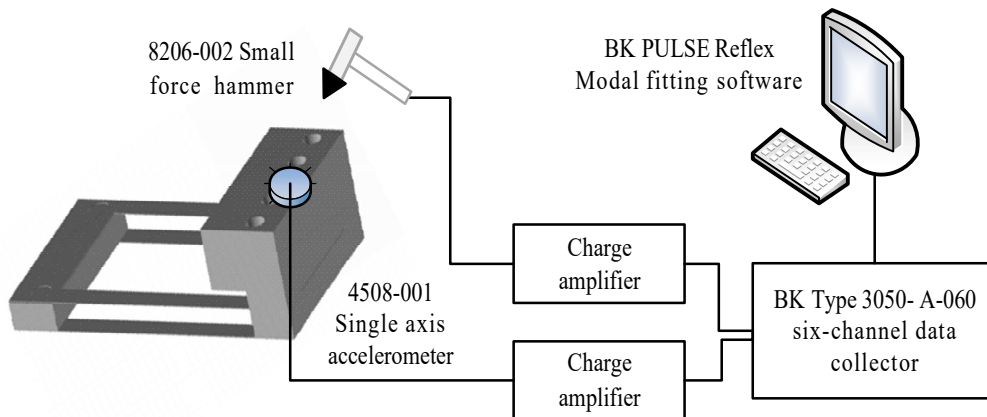
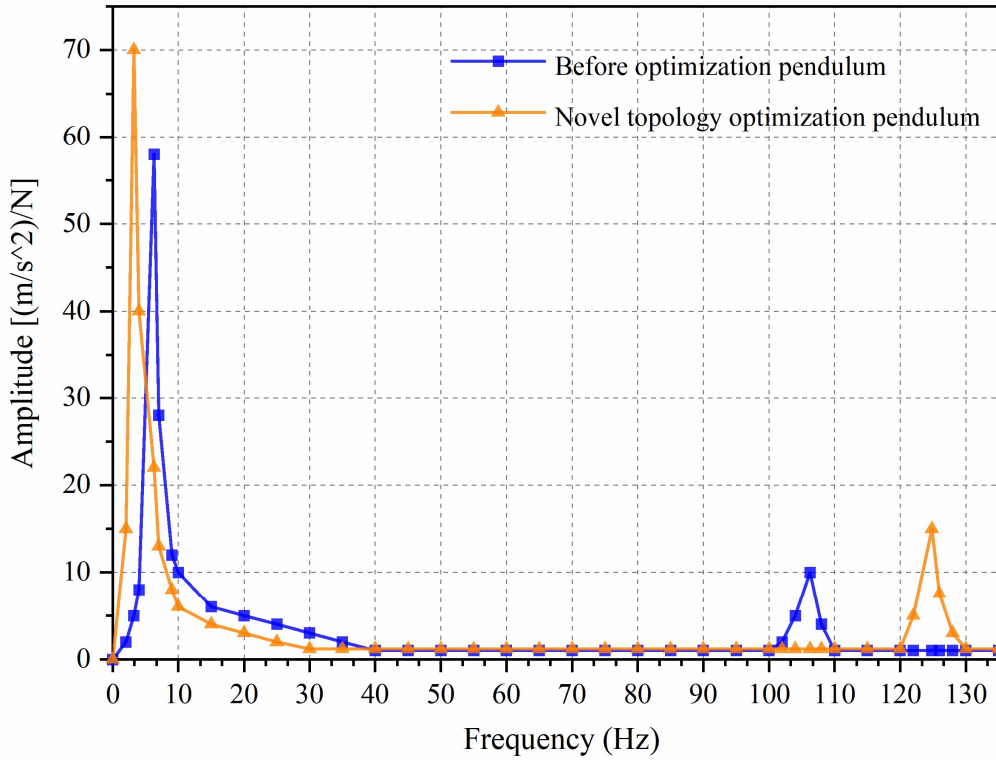


Fig. 9. The hardware set diagram for mode test experiment

The modal testing measurement experimental results of novel topology optimization pendulum and before optimization pendulum are compared in Fig. 10. The blue line is measurement experimental result of before optimization pendulum, and the orange line is measurement experimental result of novel topology optimization pendulum. The experimental results show that the maximum output signal of novel topology optimization pendulum is 3.23Hz represented with natural frequency. And the maximum output signal of before optimization pendulum is 6.30Hz as its natural frequency. As well as the spurious frequency of novel topology optimization pendulum and before optimization one with the second maximum output signal are 124.83Hz and 106.24Hz, respectively. Compared with before optimization structure pendulum, the natural frequency of novel topology optimization pendulum has reduced by about 48.73%, as well as the spurious frequency has increased by 17.50%.



249
250 **Fig. 10.** Frequency response experimental results of two kinds of pendulum

251 In the meantime, simulation and measurement experimental results of natural frequency and spurious
252 frequency characteristics with two pendulum structures are compared in Table 2. Compared with finite
253 element simulation analysis, the measurement experimental results of natural frequency and spurious
254 frequency characteristics of two pendulum structures has error within 0.96%. This verifies validity of
255 simulation model establishment and frequency characteristic analysis results.

256 **Table 2** Frequency comparison of the novel optimization pendulum and before optimization pendulum.

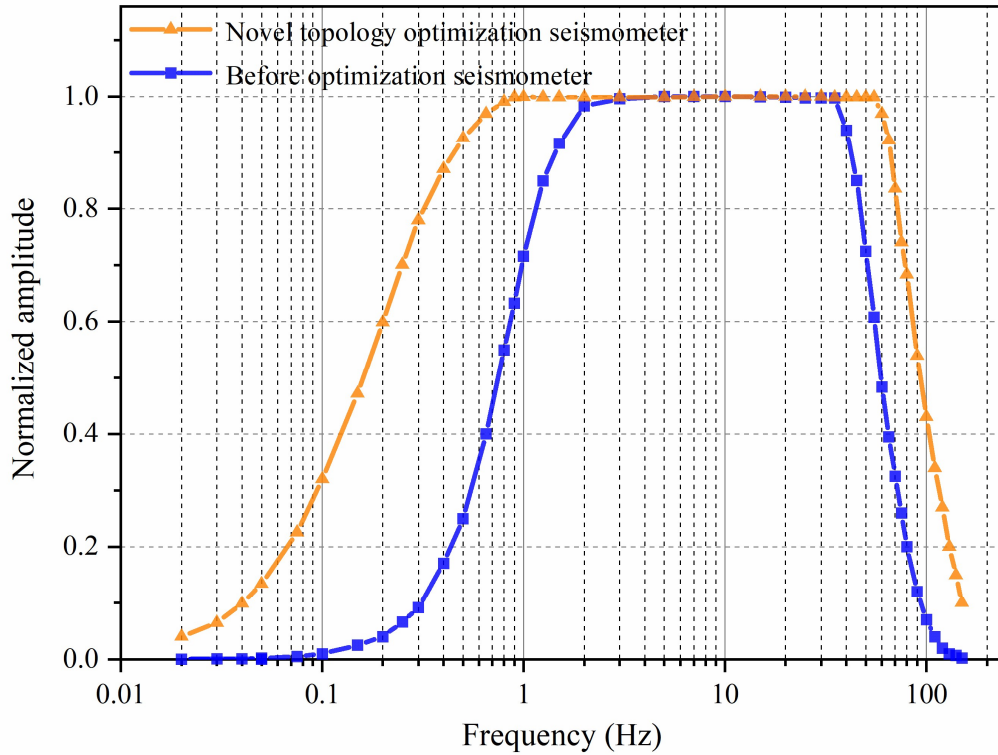
	Frequency value of before optimization pendulum (Hz)		Frequency value of novel optimization pendulum (Hz)	
	Natural frequency	Spurious frequency	Natural frequency	Spurious frequency
Simulation	6.24	105.47	3.21	124.14
Experiment	6.30	106.24	3.23	124.83
Error	0.96%	0.73%	0.62%	0.56%

257 **7.2 Shaking table test experiments**

258 To analyze the effective frequency bandwidth of seismometer influenced by the natural frequency and

259 spurious frequency of pendulum, we test the amplitude frequency characteristics of seismometer by shaking
260 table test measurement experiments conducted in Hebei key laboratory of seismic disaster instrument and
261 monitoring technology. In measurement experiments, the seismometer is fixed on the ultra-low frequency
262 standard vibration platform. Its frequency range is 0.0002-160Hz, the maximum velocity is 0.1m/s, and the
263 maximum displacement is 0.15m. Sinusoidal signals amplified by the power amplifier to drive the standard
264 shaking table, which are measured by the novel optimization seismometer. The amplitude of input sinusoidal
265 signal is 0.5cm/s, and its frequency is 0.01-150Hz.

266 Figure 11 illustrates the shaking table test measurement experimental results of novel optimization
267 seismometer and before optimization seismometer, the blue line is amplitude frequency characteristics of
268 before optimization seismometer, and the orange line is amplitude frequency characteristics of novel
269 optimization structure seismometer. The horizontal axis is the frequency of input sine vibration signals (in
270 hertz), and the vertical axis is the normalized output amplitude. From Fig.11, it can be seen that the 3dB
271 effective frequency bandwidth of novel seismometer is expanded with the topology optimization leaf spring
272 from 1s-51Hz to 4s-78Hz, which is 55.50% higher than before optimization seismometer. So the effective
273 frequency bandwidth of the novel seismometer with topology optimization leaf spring has
274 improvement.



275

276 **Fig. 11.** Vibration measurement experimental results of novel optimization seismometer and before optimization seismometer

277 **8. Conclusions**

278 The leaf spring structure is a key factor that affects effective frequency bandwidth performance of the
 279 seismometer. This paper has demonstrated that using novel topology optimization structure can expand
 280 effective frequency bandwidth of seismometer with lower natural frequency and higher spurious frequency
 281 of pendulum. Finite element simulation experiments using ANSYS Workbench show that, compared with
 282 before optimization structure pendulum, the natural frequency of novel topology optimization pendulum has
 283 reduced by about 48.55%, as well as the spurious frequency of novel topology optimization pendulum has
 284 increased 17.70%. The real vibration measurement experimental results indict that the frequency bandwidth
 285 of topology optimization seismometer is improved to [4s, 78Hz] with an increase of 55.50% over before
 286 optimization seismometer frequency bandwidth of [1s, 51Hz]. In the future, the sensitivity of a seismometer
 287 using the proposed novel topology optimization structure will be analyzed.

288 **CRedit authorship contribution statement**

289 **Zhenjing Yao:** Supervision, Methodology, Writing - review & editing. **Jingyi Zhang:** Conceptualization, Data
290 curation, Writing - original draft. **Zhitao Gao:** Data curation, Formal analysis, Investigation. **Yaran Liu and Mingyang**
291 **Li:** Software, Investigation, Validation.

292 **Declaration of Competing Interest**

293 The authors declare that they have no known competing financial interests or personal relationships that could have
294 appeared to influence the work reported in this paper.

295 **Acknowledgments**

296 This work is supported by the Special Fund of Fundamental Scientific Research Business Expense for Higher School
297 of Central Government (Projects for creation teams) (Grant No. ZY20215101), and the National Natural Science
298 Foundation of China (Grant No. 60475028). The research work of this paper is performed at Hebei Key Laboratory of
299 Seismic Disaster Instrument and Monitoring Technology.

300 **References**

- 301 [1] G.L Li, J.B Wang, D.Y Chen, *et al.*, An Electrochemical, Low-frequency seismic micro-sensor based on MEMS with
302 a force-balanced feedback system, *Sensors*. 17 (9) (2017) 2103, <http://dx.doi.org/10.3390/s17092103>.
- 303 [2] J. Lin, H. Gao, X.F. Wang, *et al.*, Effect of temperature on the performance of electrochemical seismic sensor and the
304 compensation method, *Measurement*. 155 (2020) 107518, <http://dx.doi.org/10.1016/j.measurement.2020.107518>.
- 305 [3] J.Y. Wang, B.X. Hu, W. Li, *et al.*, Design and application of fiber Bragg grating (FBG) geophone for higher
306 sensitivity and wider frequency range, *Measurement*. 79 (2016) 228-235,
307 <http://dx.doi.org/10.1016/j.measurement.2015.09.041>.
- 308 [4] X.L. Zhang, X.M. Liu, F.X. Zhang, *et al.*, Reliable high sensitivity FBG geophone for low frequency seismic
309 acquisition, *Measurement*. 129 (2018) 62-67, <http://dx.doi.org/10.1016/j.measurement.2018.07.009>.
- 310 [5] Y.T Teng, X.X Hua, H.Y Lu, Research on magnetoelectric seismometer's low frequency extension technology, *Appl.*
311 *Mech. Mater.* 664 (2014) 268-273, <http://dx.doi.org/10.4028/www.scientific.net/AMM.664.268>.
- 312 [6] K. Faber, P.W. Maxwell, Geophone spurious frequency: What is it and how does it affect seismic data quality, *Can. J.*
313 *Explor. Geophys.* 33 (1-2) (1997) 46-54, <http://dx.doi.org/10.1190/1.1826773>.
- 314 [7] D.M. Woo, Geophone spring, U.S. patent 5,134,594, (1992).
- 315 [8] E. Wielandt, G. Streckeisen, The leaf-spring seismometer: Design and performance, *Bull. Seismol. Soc. Am.* 72 (6)
316 (1982) 2349-2367.
- 317 [9] D.P. Yang, N.R. Li, C.Y. Liu, *et al.*, Note: Improving the performance of a geophone through suspension system
318 configuration, *Rev. Sci. Instrum.* 85 (12) (2014) 84-92, <http://dx.doi.org/10.1063/1.4897183>.

- 319 [10] Y. Xin, H.S. Sun, C. Guo, *et al.*, Note: A novel optimization cantilever beam for low frequency high performance
320 piezoelectric geophone, *Rev. Sci. Instrum.* 88 (6) (2017) 066105-1-066105-3, <http://dx.doi.org/10.1063/1.4986810>.
- 321 [11] Z.J. Yao, Y.L. Duan, L.L. Li, *et al.*, Bandwidth extension of seismometer by using a novel topology leaf spring, *Rev.*
322 *Sci. Instrum.* 90 (7) (2019) 076109-1-076109-3, <http://dx.doi.org/10.1063/1.5097026>.
- 323 [12] I. Muramatsu, T. Sasatani, I. Yokoi, Velocity-type strong-motion seismometer using a coupled pendulum: Design
324 and Performance, *Bull. Seismol. Soc. Am.* 91 (3) (2001) 604-616, <http://dx.doi.org/10.1785/0120000023>.
- 325 [13] O. Sigmund, K. Maute, Topology optimization approaches, *Struct. Multidisc. Optim.* 48 (6) (2013) 1031-1055,
326 <http://dx.doi.org/10.1007/s00158-013-0978-6>.
- 327 [14] H.A. Eschenauer, N. Olhoff, Topology optimization of continuum structures: A review, *Appl. Mech. Rev.* 54 (4)
328 (2001) 331-389, <http://dx.doi.org/10.1115/1.1388075>.
- 329 [15] W.J. Zuo, K. Saitou, Multi-material topology optimization using ordered SIMP interpolation, *Struct. Multidisc.*
330 *Optim.* 55 (2) (2016) 477-491, <http://dx.doi.org/10.1007/s00158-016-1513-3>.
- 331 [16] W.M. Vicente, Z.H. Zuo, R. Pavanello, *et al.*, Concurrent topology optimization for minimizing frequency responses
332 of two-level hierarchical structures, *Comput. Methods Appl. Mech. Engrg.* 301 (2016) 116-136,
333 <http://dx.doi.org/10.1016/j.cma.2015.12.012>.
- 334 [17] Z.D. Li, X.J. Liu, Guide-weight method on solving topology optimization problems under single load case, *J. Mech.*
335 *Eng.* 47 (15) (2011) 107-114, <http://dx.doi.org/10.3901/JME.2011.15.107>.
- 336 [18] K. Svanberg, The method of moving asymptotes – a new method for structural optimization, *Int. J. Numer. Meth.*
337 *Eng.* 24 (2) (1987) 359-373, <http://dx.doi.org/10.1002/nme.1620240207>.
- 338 [19] K. Svanberg, A class of globally convergent optimization methods based on conservative convex separable
339 approximations, *SIAM J. Optimiz.* 12 (2) (2002) 555-573, <http://dx.doi.org/10.1137/S1052623499362822>.
- 340 [20] Y. Okamoto, R. Hoshino, S. Wakao, *et al.*, Improvement of torque characteristics for a synchronous reluctance
341 motor using MMA-based topology optimization method, *IEEE Trans. Magn.* 54 (3) (2018) 1-4,
342 <http://dx.doi.org/10.1109/TMAG.2017.2762000>.